GEOPHYSICS, VOL. 72, NO. 4 (JULY-AUGUST 2007); P. E119–E123, 5 FIGS.
10.1190/1.2734382

Stop-go temperature logging for precision applications

Robert N. Harris[1] and David S. Chapman[2]

ABSTRACT

We describe a new field procedure for stop-go temperature logging of boreholes that attains millikelvin precision. Temperature is recorded continuously throughout the entire log, but the logging probe is held stationary for a fixed time at discrete depth intervals. Equilibrium temperatures at the discrete depths are based on extrapolations of time series using the heat-diffusion theory for an infinitely long cylinder. For a Fenwahl K212E thermistor probe having a time constant of about 7 s, temperatures are still 6 mK away from equilibrium after a wait time of 30 s; but temperatures extrapolated from the time series are within 2 mK of equilibrium. A time series over a duration of seven time constants of the probe allows the user to reproduce temperature estimates within millikelvins. The technique was applied at GC-1, a borehole in northwestern Utah.

INTRODUCTION

Borehole temperature profiles contain a rich source of information concerning subsurface and surface thermal properties. Subsurface processes affecting temperature profiles include variations in thermal conductivity (e.g., Blackwell et al., 1999), coupled heat and fluid flow through porous and fractured rocks (e.g., Smith and Chapman, 1983; Drury et al., 1984; Ge, 1998; Constanz et al., 2003), and detection of shear heating along faults or at the base of ice sheets (Safanda et al., 2004; Yasuyuki et al., 2006). Surface processes affecting temperature profiles include topography, differential solar radiation, vegetation, and past changes in surface temperature (see Appendix A in Chisholm and Chapman, 1992; Harris and Chapman, 1995). In addition, temperature logs are becoming increasingly important in environmental applications and are useful for assessing excess heat associated with radioactive waste storage and fluid movement associated with casing integrity.

Exploiting this information fully requires high-precision measurements of temperature and the ability to separate noise from small but meaningful variations in temperature. High precision is especially important because temperature logs increasingly are being made for detecting temporal, rather than spatial variations in the thermal field. Perhaps nowhere is the need for high-precision temperature logs greater than when they are used to reconstruct histories of ground-surface temperature for studies of climate change. Application of Backus-Gilbert inverse theory to interpretations of temperature-depth profiles in terms of ground-surface temperature histories demonstrates that our ability to resolve past climatic events can be optimized by reducing the random errors in the temperature measurement to no more than 0.1% of the climate signal being sought (Clow, 1992).

Precision temperature logs differ from other open-hole logs in two respects. First, precision temperature logs need to be measured in holes that are in near-thermal equilibrium, such that a relaxation time after drilling, production, and other logging is needed. A second difference between temperature logs and other open-hole logs is that, whereas most logging tools collect measurements on the way up, precision temperature logs need to be collected on the way down so that the measuring environment is not disturbed prior to introducing the temperature tool. Both of these considerations require a separate logging trip for precise temperature measurement.

Two modes of temperature logging techniques are conventionally used (e.g., Jessop, 1990). In the first method, known as stop-go or incremental logging (Beck, 1965; Costain, 1970), the temperature probe is lowered to the depth of interest, and after some time interval passes, the temperature is recorded. This method results in a series of temperature measurements at discrete depths. In the second method, known as continuous logging (e.g., Costain, 1970; Conaway and Beck, 1977; Conaway, 1977), the probe is lowered at a constant speed, with the measurements limited by the sampling rate. However, the time response of the probe must be deconvolved from the measurements (Conaway, 1977; Saltus and Clow, 1994), and slip-ring noise may introduce uncertainties.

In this paper, we show that a hybrid combination of these techniques — continuous recording while stopping at discrete depths —

Manuscript received by the Editor November 12, 2006; revised manuscript received February 25, 2007; published online May 23, 2007.
[1]Oregon State University, College of Oceanic and Atmospheric Sciences, Corvallis, Oregon. E-mail: rharris@coas.oregonstate.edu.
[2]University of Utah, Department of Geology and Geophysics, Salt Lake City, Utah. E-mail: chapman@earth.utah.edu.

can produce high-quality temperature-depth profiles with millikelvin temperature precision. Our technique consists of stopping the probe at discrete depths as in the stop-go technique, but continuously record temperature at 0.5 s intervals as with continuous logs. The recorded time series is used to extrapolate to an equilibrium temperature.

TEMPERATURE MEASUREMENT

We measure borehole temperature using a Fenwahl K212E thermistor probe based on the design of Sass et al. (1971). The tool consists of a thin probe protruding from a 2.22-cm-diameter, 20-cm-long brass cylinder within which the four-wire logging cable is attached to the probe. The stainless steel probe is 2 mm in diameter and 12 cm long; it contains two arrays of 20 negative-temperature-coefficient (NTC) thermistors hermetically sealed in glass. This design is favored because of its ruggedness, stability, and high sensitivity to temperature (Clow et al., 1996). Arrays of thermistor beads minimize self-heating effects, and hermetically sealing the beads in glass improves long-term stability by minimizing oxides that would otherwise form on the ceramic beads. The time constant for our probe in still water is 7 s. Our probes are routinely calibrated against a Hewlett Packard model 2804a quartz thermometer. Misfits of individual calibration points to a calibration curve suggest that our temperature accuracy is 30 mK (Chisholm and Chapman, 1992).

Resistances are measured in a four-wire configuration via a digital multimeter at the surface (Beck and Balling, 1988). In the field, thermistor resistances are measured to ±1 Ω, which, for our 10-kΩ probes, translates to a temperature precision of ±2.5 mK. Precision of ±0.2 mK is possible by using a resistance meter that measures reliably to 0.1 Ω. A slip-ring assembly provides electrical continuity between the logging cable and the surface electronics. Depths in the hole are measured with a Veeder-Root measuring wheel and counter. The probe can be positioned to ±0.1 wheel revolution, or ±0.03 m. A positioning uncertainty of 3 cm is equivalent to a temperature uncertainty of 1 mK in a typical continental setting having a geothermal gradient of 30 mK/m. Cable stretch or hysteresis in the measuring wheel should not introduce significant errors in the temperature measurements. A laptop computer stores the three data streams needed: thermistor depth, resistance, and time.

THEORY

We draw on a method used extensively in computing equilibrium temperatures from marine heat-flow probes where minimizing the measurement time is important (e.g., Davis and Villinger, 1987). Equilibrium temperatures can be estimated by using the theory of radial heat diffusion for an infinitely long, perfectly conducting cylinder subjected to a step change in temperature (Jaeger, 1956; Carslaw and Jaeger, 1959). The temperature response $T(t)$ to an instantaneous temperature change ΔT is described by the function $F(\alpha, \tau)$ (Bullard, 1954),

$$T(t) = T(\infty) - \Delta T F(\alpha, \tau), \tag{1}$$

where $T(\infty)$ is the new equilibrium temperature and ΔT is the temperature step.

The function $F(\alpha, \tau)$ can be expressed as (Bullard, 1954)

$$F(\alpha, \tau) = \frac{4\alpha}{\pi^2} \int_0^\infty \frac{\exp(-\tau u^2)}{u \Delta u} du, \tag{2}$$

where

$$\Delta u = [uJ_0(u) - \alpha J_1(u)]^2 + [uY_0(u) - \alpha Y_1(u)]^2 \tag{3}$$

and where J_n and Y_n are Bessel functions of order n of the first and second kind, respectively. In these equations, the first argument, α is twice the ratio of the heat capacity of the fluid ρc being displaced by the probe to the heat capacity of the probe S, such that

$$\alpha = 2\pi a^2 \frac{\rho c}{S} \tag{4}$$

and a is the probe radius. The second argument τ is a dimensionless time that can be expressed as

$$\tau = \frac{\kappa t}{a^2}, \tag{5}$$

where κ is the diffusivity of the medium ($k/\rho c$), k is the thermal conductivity, and t is the elapsed time since the disturbance. In equations 1 and 2, $F(\alpha,0) = 1$ and $F(\alpha, \infty) = 0$. Equilibrium temperatures are computed by a least-squares fit to the cylindrical decay, and the equilibrium temperature is the y-intercept (equation 1) on a plot of $T(t)$ versus $F(\alpha, \tau)$.

FIELD RESULTS

We tested our procedure in a 150-m-deep borehole in northwestern Utah (GC-1) that has been logged repeatedly since 1978 (Chapman and Harris, 1993). GC-1 is on the south flank of the Grouse Creek Mountains in northwest Utah and was drilled into a granitic pluton in an area specifically chosen to minimize thermal perturbations caused by rock inhomogeneity and topographic effects. The 150-mm-diameter borehole was completed by inserting a bottom-capped, 64-mm-inner-diameter PVC pipe, and the annulus was backfilled with a slurry of drill cuttings. In 1993, we inserted a second PVC pipe, with an inner diameter of 25 mm, inside the 64-mm pipe. Baffles were attached to the outside of the small-diameter pipe to damp potential convection of the water in the annulus between the inner and outer plastic pipes.

In 2002, a sequence of three temperature logs was collected over a three-day period, one on each successive day. Figure 1 shows the temperature-time series for the first hybrid log between depths of 20 and 29 m. Each segment in this figure shows (1) the rise in temperature caused by the geothermal gradient as the probe descends between measurement depths and (2) an apparent plateau in temperature as the probe is held at a specified depth and tries to equilibrate to a new temperature. Temperatures are recorded approximately every 0.5 s, the lowering time between specified depths is 5–15 s, and the probe is held at each depth for approximately 70 s, corresponding to 10 time constants.

Temperatures corresponding to the lowering and holding of the probe at each depth are separated into segments, based on the probe velocity, and plotted against relative time (Figure 2a). The initial rise in temperature as the probe is being lowered and the asymptotic approach to a new equilibrium temperature are evident. The different behavior of the temperature rise at each depth reflects the details of

the acceleration, speed, and deceleration of the probe as it is lowered by hand. Temperatures as a function of $F(\alpha,\tau)$ for those same depths are plotted in Figure 2b. We exclude the first 7 s corresponding to the time constant of the probe and compute the equilibrium temperatures by determining the least-squares intercept temperature. These intercepts are well determined with standard deviations of less than 1 mK. The distance between the temperatures and the dashed line for each depth in Figure 2a provides an estimate of the deviation from equilibrium as a function of time.

In the marine heat-flow literature (e.g., Villinger and Davis, 1987; Hartman and Villinger, 2002), considerable attention has been paid to problems associated with not knowing the precise origin time for the start of the thermal decay. The optimum origin time is usually chosen as the value that minimizes the standard deviation of the linear fit to the $F(\alpha,\tau)$ series (Villinger and Davis, 1987). We tested our sensitivity to the origin time following the same procedure of optimizing the linear fit to the transformed temperature data. Our results suggest that a sharp acceleration in the probe at the beginning of each lowering provides the best-resolved minima in the rms misfit. In some cases, this procedure suggested a time shift of 5 s; but even with this large time shift, changes in the equilibrium temperature are less than 1 mK. For our application, we do not consider potential time shifts further.

Figure 3 demonstrates one advantage of the stop-go logging method and use of $F(\alpha,\tau)$ by showing histograms of the temperature difference between observed and equilibrium temperatures after wait times of 30 and 60 s. After a 30-s wait (Figure 3a), temperatures on average are 6 mK shy of the equilibrium temperature, although the variation is considerable, 1 to 10 mK. After a 60-s wait (Figure 3b), both the temperature difference and scatter are reduced. The mean difference is 4 mK, and the range is only 1–6 mK.

The advantage of using a time-series $F(\alpha,\tau)$ extrapolation rather than a single time measurement is illustrated in Figure 4. The plot is constructed by using progressively longer time series, in multiples of the probe time constant (7 s), and comparing the extrapolated $T(\infty)$ from the truncated time series with $T(\infty)$ estimated by using the full approximately 70-s data stream. Using $F(\alpha,\tau)$ allows us to estimate equilibrium temperature within 2 mK for a 30-s time series; a 49-s time series (seven time constants) yields equilibrium temperature estimates within 1 mK of the true equilibrium temperature. Our results show that an appropriate waiting time at each depth is approximately seven time constants. Faster platinum-resistance transducers, however, may shorten the required time between stops.

Millikelvin precision is important because, even at this accuracy, repeatable signals may exist that would otherwise be interpreted as noise. Figure 5 shows a comparison of three temperature logs collected over the three-day period in 2002. To accentuate the consistency and variability between the logs, we plot temperatures between 100 and 150 m, at an expanded temperature scale, by removing the background gradient (31.05°C/km) and surface-temperature intercept (10.68 °C). The most important feature of the millikelvin-precision logs is a repeatable, fine structure to the temperature profile that would have been interpreted as noise at the 10-mK level. Root-mean-square differences, computed point by point, between logs 1 and 2, 1 and 3, and 2 and 3 are 5, 3, and 4 mK, respectively. The maximum difference in temperature between any two depths is 10 mK.

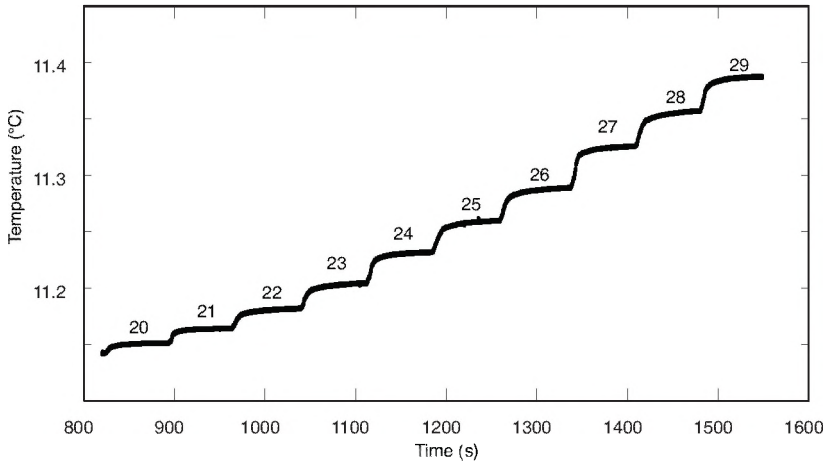

Figure 1. Stop-go temperature logging of borehole GC-1 in northwestern Utah. Temperatures are recorded every 0.5 s. The probe is lowered by the 1-m logging interval for 5–15 s and is then left stationary for about 60 s. Data for depths between 20 and 29 m (as labeled) are shown.

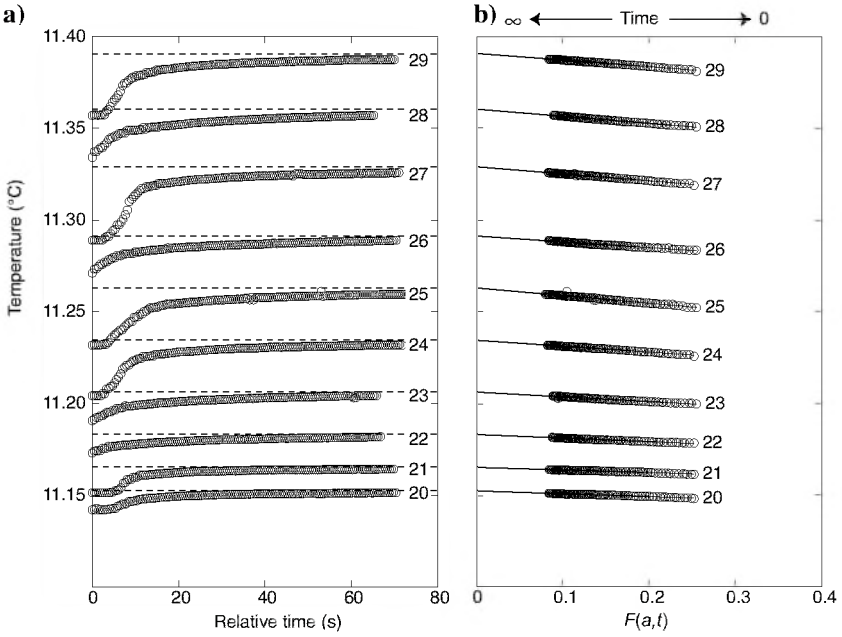

Figure 2. Illustration of the $F(\alpha,\tau)$ method. (a) Temperature-time series for each depth are shown as a function of relative time. Dashed line shows computed equilibrium temperature. (b) $F(\alpha,\tau)$ series for each depth. Line shows best-fitting solution; equilibrium temperatures are the intercepts.

The differences between the reduced-temperature profiles show a coherent structure to the temperature variations in the borehole. The most likely causes of these temperature perturbations are either variations in thermal conductivity or convective instabilities in the cased borehole or outside the casing (Chapman and Harris, 1993). If convection is responsible for the fine temperature structure, the convection is spatially locked, perhaps by heterogeneities in thermal properties or by slight variations in drill-hole diameter.

The test data set used in this analysis is from a thermally stable borehole. Efforts to damp convection within the borehole included

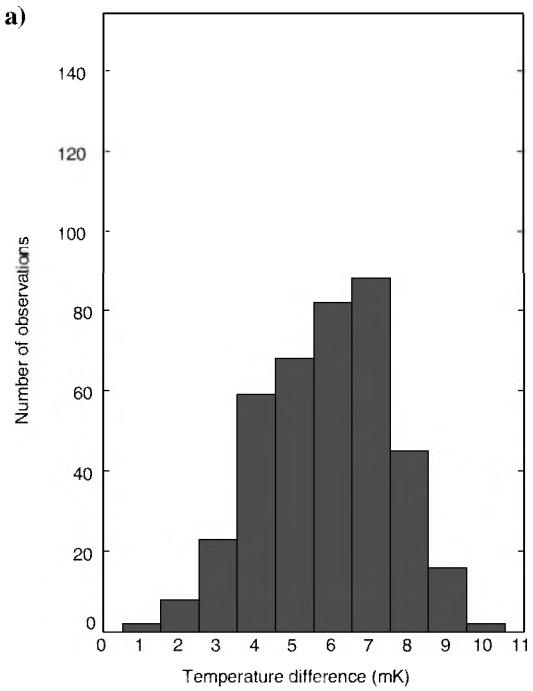

Figure 3. Histograms of temperature differences between computed equilibrium temperatures and observed temperatures at wait times of (a) 30 and (b) 60 s.

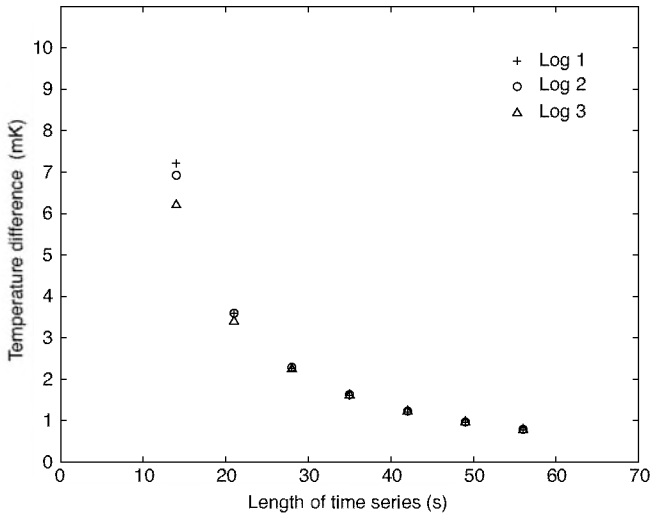

Figure 4. Benefits of the $F(\alpha, \tau)$ method. The difference between equilibrium temperatures computed from the entire time series and computed by using a shorter truncated time series at each depth are plotted against the length of truncated time series used. The plot is constructed at multiples of the probe time constant (7 s). Points show average difference from 20 to 150 m.

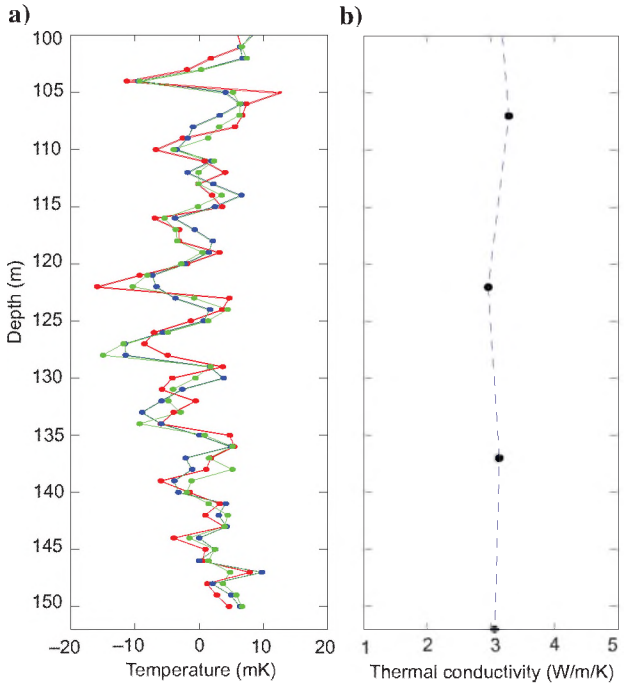

Figure 5. (a) Reduced temperatures for GC-1 between 100 and 150 m, showing consistency of temperature measurements at each depth. (b) Thermal conductivity of the granite pluton is uniform at the scale sampled.

measuring in a water-filled borehole and inserting a small-diameter pipe with baffles around the outside of the inner annulus to damp convection. In larger-diameter boreholes or open holes, vertical convection may be expected, and this technique may provide a diagnostic test of advective heat transfer. For example, in a 0.2-m-diameter borehole, convection may be on the scale of a few borehole diameters, or 0.6 m. A standard continental gradient of 30 mK/m would yield a temperature disturbance of 18 mK. Small-scale convection may be manifested as noise in $F(\alpha,\tau)$ plots, poor statistics, or a variable slope in $F(\alpha,\tau)$ plots. Although the results presented here represent a small but significant improvement in repeatability, this technique is likely to be helpful in discerning between noise and signal in harsh measuring environments represented by large-diameter boreholes or boreholes filled with air.

CONCLUSIONS

The hybrid temperature of stop-go logging while continuously recording temperature affords high precision without sacrificing efficiency or time required to log a borehole. This technique is implemented easily by using inexpensive portable borehole logging equipment. A temperature time series of 60 s acquired at each depth yields millikelvin precision. The procedure should be particularly useful in detecting small changes in borehole temperatures associated with climate change, frictional heating of faults, or subtle hydrogeologic effects.

ACKNOWLEDGMENTS

This research was funded by National Science Foundation grants EAR-0545342 and EAR 0126026. We thank three anonymous reviews and the associate editor for comments that improved this manuscript.

REFERENCES

Beck, A. E., 1965, Techniques of measuring heat flow on land, *in* W. H. K. Lee, ed., Terrestrial heat flow: American Geophysical Union Geophysical Monographs 8, 24–57.

Beck, A. E., and N. Balling, 1988, Determination of virgin rock temperatures, *in* R. Haenel, L. Rybach, and L. Stegena, eds., Handbook of terrestrial heat-flow density determination: Kluwer Academic Publishers, 59–85.

Blackwell, D. D., G. R. Beardsmore, R. K. Nishimori, and M. J. McMullen, Jr., 1999, High-resolution temperature logs in a petroleum setting, examples and applications, *in* D. Merriam and A. Förster, eds., Geothermics in basin analysis: Kluwer Academic Publishers, 1–33.

Bullard, E. C., 1954, The flow of heat through the floor of the Atlantic Ocean: Royal Society of London Proceedings, ser. A, **222**, 408–429.

Carslaw, H. S., and J. C. Jaeger, 1959, Conduction of heat in solids, 2nd ed.: Oxford University Press.

Chapman, D. S., and R. N. Harris, 1993, Repeat temperature measurements in borehole GC-1, northwestern Utah: Towards isolating a climate-change signal in borehole temperature profiles: Geophysical Research Letters, **18**, 1891–1894.

Chisholm, T. J., and D. S. Chapman, 1992, Climate change inferred from analysis of borehole temperatures: An example from western Utah: Journal of Geophysical Research, **97**, 14,155–14,175.

Clow, G. D., 1992, The extent of temporal smearing in surface-temperature histories derived from borehole temperature measurements: Palaeogeography, Palaeoclimatology, Palaeoecology, **98**, 81–86.

Clow, G. D., R. W. Saltus, and E. D. Waddington, 1996, A new high-precision borehole-temperature logging system used at GISP2, Greenland, and Taylor Dome, Antarctica: Journal of Glaciology, **42**, 576–584.

Conaway, J. G., 1977, Deconvolution of temperature gradient logs: Geophysics, **42**, 823–837.

Conaway, J. G., and A. E. Beck, 1977, Continuous logging of temperature gradients: Tectonophysics, **41**, 1–7.

Constantz, J., S. W. Tyler, and E. Kwicklis, 2003, Temperature-profile methods for estimating percolation rates in arid environments: Vadose Zone Journal **2**, 12–24.

Costain, J. K., 1970, Probe response and continuous temperature measurements: Journal of Geophysical Research, **75**, 3969–3975.

Davis, E. E., and H. Villinger, 1987, Journal of Geophysical Research, **92**, 12,846–12,856

Drury, M. J., A. M. Jessop, and T. J. Lewis, 1984, The detection of groundwater flow by precise temperature measurements in boreholes: Geothermics, **13**, 163–174.

Ge, S., 1998, Estimation of groundwater velocity in localized fracture zones from well temperature profiles: Journal of Volcanology and Geothermal Research, **84**, 93–101.

Harris, R. N., and D. S. Chapman, 1995, Inferring surface ground temperature histories from borehole temperature measurements in the Colorado Plateau of eastern Utah: Journal of Geophysical Research, **100**, 6367–6381.

Hartmann, A., and H. Villinger, 2002, Inversion of marine heat flow measurements by expansion of the temperature decay function: Geophysical Journal International, **148**, 628–636.

Jaeger, J. C., 1956, Conduction of heat in an infinite region bounded internally by a circular cylinder of a perfect conductor: Australian Journal of Physics, **9**, 167–179.

Jessop, A. M., 1990, Thermal geophysics: Elsevier Science Publ. Co., Inc.

Safanda, J., J. Szewczyk, and J. Majorowicz, 2004, Geothermal evidence of very low glacial temperatures on a rim of the Fennoscandian ice sheet: Geophysical Research Letters, **31**, L07211; http://dx.doi.org/10.1029/2004GL019547.

Saltus, R. W., and G. D. Clow, 1994, Deconvolution of continuous borehole temperature logs: Example from the Greenland GISP2 icecore hole: U. S. Geological Survey Open-File Report OF 94-0254.

Sass, J. H., A. H. Lachenbruch, R. J. Munroe, G. W. Greene, and T. H. Moses, Jr., 1971, Heat flow in the western United States: Journal of Geophysical Research, **76**, 6376–6413.

Smith, L., and D. S. Chapman, 1983, On the thermal aspects of groundwater flow 1: Regional scale systems: Journal of Geophysical Research, **88**, 593–608.

Villinger, H., and E. E. Davis, 1987, A new reduction algorithm for marine heat flow measurements: Journal of Geophysical Research, **92**, 12846–12856.

Yasuyuki, K., J. Mori, R. Fujio, H. Ito, T. Yanagidani, S. Nakao, and K. Ma, 2006, Heat signature on the Chelungpu fault associated with the 1999 Chi-Chi, Taiwan earthquake: Geophysical Research Letters, **33**, L14306; http://dx.doi.org/10.1029/2006GL026733.